


Article

An Improved Simplified Urban Storm Inundation Model Based on Urban Terrain and Catchment Modification

Yao Li ¹, Tangao Hu ^{1,*} , Gang Zheng ², Lida Shen ¹, Jinjin Fan ¹ and Dengrong Zhang ¹

¹ Zhejiang Provincial Key Laboratory of Urban Wetlands and Regional Change, Hangzhou Normal University, Hangzhou 311121, China; yaoli_sofia@163.com (Y.L.); sld1031@163.com (L.S.); fanjinjin0608@163.com (J.F.); zju_rs@126.com (D.Z.)

² The State Key Laboratory of Satellite Ocean Environment Dynamics, Second Institute of Oceanography, Ministry of Natural Resources, Hangzhou 310012, China; zhenggang@sio.org.cn

* Correspondence: hutangao@hznu.edu.cn; Tel.: +86-138-5712-3496

Received: 20 September 2019; Accepted: 4 November 2019; Published: 7 November 2019



Abstract: Flooding caused by unpredictable high-intensity rainfall events in urban areas has become a global phenomenon due to the combined effect of urbanization and climate change. There are numerous hydrodynamic models for urban flooding simulation and management. However, it is difficult for most of these models to simplify the surface runoff process and still provide high simulation accuracy. In this study, an improved simplified urban storm inundation model (SUSIM) that integrates urban terrain, precipitation, surface runoff and inundation models was proposed to quickly and accurately simulate the different inundation conditions by modifying the urban terrain and catchments. Haining City, China, was selected as a case study in which SUSIM was tested and validated. The results were as follows: (1) Detailed locations and depths of inundation were quickly calculated with high correlation coefficient ($\geq 75\%$) compared to three actual rainfall events. (2) Four scenarios under different rainfall intensities (5-, 10-, 20- and 50-year return period, respectively) were designed. The maximum inundation depths significantly increased from 403 mm to 1522 mm and the maximum inundation area increased from 2904 m² to 7330 m². According to the simulation results, Haining Avenue, the West Mountain Park and the old urban area in the northeast part of the city would encounter the most extensive and severe inundation. The result reveals that the SUSIM could find inundation locations and calculate inundation depth and area quickly. It provides better insights and tools for urban inundation simulation and planning strategies.

Keywords: simplified urban storm inundation model; urban terrain modification; contributing areas of depressions; inundation projection; Haining City

1. Introduction

As the global climate changes and rapid urbanization progresses, the frequency and intensity of natural hazards are increasing because of interactions between natural and artificial factors [1,2]. The problems caused by urban expansion are becoming increasingly prominent, especially urban flooding and inundation caused by heavy rainfall in the flood season, which has been an urgent problem that requires solutions in most cities [3]. Urban flooding is one of the most severe hazards and can cause enormous human and societal economic losses [4]. For example, the heavy rainfall (460 mm of rainfall in 24 h) recorded at a hydrological station in Beijing on 21–22 July 2012 caused at least 79 deaths and affected more than 1.9 million people [5]. Consequently, urban flooding and inundation issues have drawn increasing attention in recent years [6]. It is essential to simulate the inundation results and evaluate the inundation risks and response in inundation management [7]. However, it will

take a long time to investigate and measure the extent of inundation and the resulting property damage using traditional field-survey approaches [8]. Therefore, an efficient urban inundation model would be a particularly significant improvement [9]. Urban storm inundation models can provide useful information for facilitating the relief process and managing infrastructure, communities and natural resources during disaster management [8]. Common urban storm simulation models include the IHDM (Institute of Hydrology Distributed Model) [10], SWMM (Storm Water Management Model) [11,12], SWAT (Soil and Water Assessment Tool) [13,14], shallow water models [15,16], and others. For these complex models like SWMM and shallow water models, SWMM requires a large number of parameters and amount of input data [17–19], shallow water models needs complicated correlative calculation [16], and the use of these large hydrology models has been limited. Another type of model that can be used in a predictive and simulative way is the Rapid Flood Inundation Method (RFIM) [20] or the Rapid Flood Spreading Method (RFSM) [21].

These simplified models require significantly less computer effort than hydrodynamic models. They are fast and robust, which is desirable for applications that have low demands for the representation and accuracy of flow dynamics. Krupka et al. [20] constructed an array of flood-storage cells from the floodplain DEM (digital elevation model) and spread a volume of floodwater over those cells. Chen et al. [22] presented an urban pluvial flood inundation model that included both storm-runoff and inundation models. Zhang et al. [23] introduced the flood-connected domain calculation (FCDC) method to simulate fluvial inundation. The method considers flow continuity and can rapidly simulate source flooding, such as inundation by river flooding or dike-breach flooding. However, these simplified models cannot actually reflect the impact of the complex urban terrain on the surface runoff, sewer runoff and inundation process.

In this study, we proposed an improved simplified urban storm inundation model (SUSIM) to simulate the depths of urban inundation under different rainstorm scenarios. The main objectives of this study are: (1) To modify the original DEM to reflect the real urban terrain and consider the impact of complex urban terrain like buildings on the surface runoff. (2) The contributing areas of depressions are the basic hydrological units and are defined as the basic units of SUSIM to reflect the real processes of flowing water and to improve the accuracy of the simulation. (3) The processes of evaporation, infiltration and sewer system drainage are simplified to increase the ease of the model run and the speed of the calculation. This study will contribute to a better understanding of urban inundation simulation, which may lead to improvements in urban management and planning strategies.

2. Simplified Urban Storm Inundation Model

2.1. Urban Terrain Model

2.1.1. Urban Terrain Modification

DEM is the foundation of SUSIM and has sufficient information to describe the continuously varying topography [24]. It is also the basis for hydrologic assessment and plays a major role in determining the accuracy of flood inundation modeling [25]. Usually, the original DEM only represents the elevation change of the exposed surface in the city. However, there is a large number of buildings of a certain height on the urban surface that make the entire surface elevation change significantly. The existence of buildings will significantly affect the diffusion process of inundation water. When simulating urban storm inundation, buildings play an important role in blocking the flow of water.

To reflect the real and complex urban terrain and consider the blocking effects of the constructions, the heights of the buildings and other constructions need to be rebuilt into the original DEM. First, the profiles of the buildings need to be derived from high spatial-resolution satellite images.

Then, the building binary raster is used to modify the original DEM based on spatial analyst tools in ArcGIS® 10.2 by ESRI (Environmental Systems Research Institute, Inc., Redlands, CA, USA). This modified process is calculated by:

$$D_{ij} = O_{ij} + A * C_{ij} \quad (i = 1, 2, \dots, n; j = 1, 2, \dots, m) \quad (1)$$

where D_{ij} denotes the final real urban surface of the grid cell in Row i and Column j . O represents the original DEM value and C represents urban building binary raster value, i and j respectively represent the i th row and j th column of the DEM raster. A stands for the height value of the building. Take a 10-m-high building for example, the modification process can be shown in Figure 1.

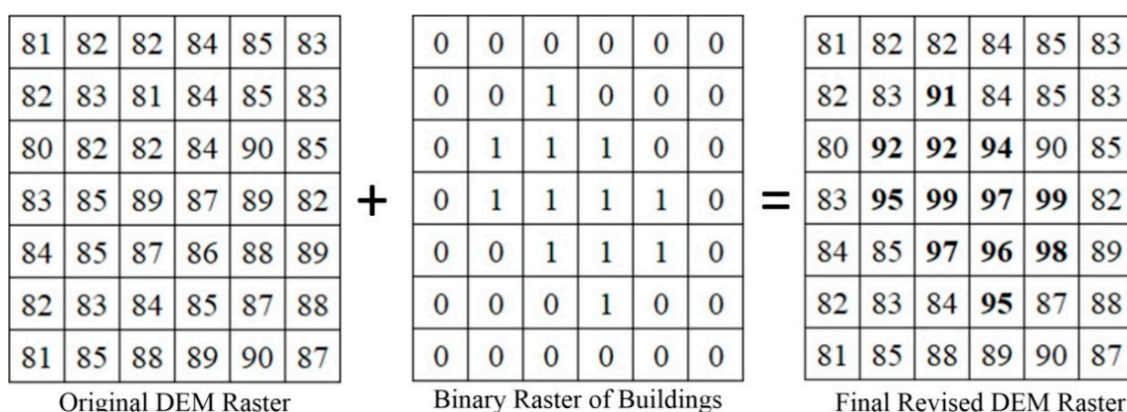


Figure 1. The process of urban terrain modification.

2.1.2. Contributing Depressions Extraction

The contributing areas of depressions as the fundamental units and the basic catchments in SUSIM can be delineated based on the modified DEM. A finer catchment can contribute to more accurate results. In this study, the basic catchments are defined as the contributing areas of depressions [26]. A depression is a cell or set of spatially connected cells in which the flow direction cannot be assigned one of the eight valid values in a flow direction raster. This can occur when all neighboring cells are higher than the cell being processed or when two cells flow into each other, creating a two-grid loop. The boundaries between catchments are termed drainage divides.

The catchments of each depression are determined as follows. First, ArcGIS hydrology tools are used to generate the flow direction raster based on the revised DEM raster. We assume that the filled DEM is the same as the area where flow fills all the depressions. Then, depressions are calculated using the filled DEM minus the original DEM; the result provides the contributing areas of depressions. In addition, the catchment boundary is modified according to the actual characteristics of the urban terrain, such as river banks and roads.

2.2. Precipitation Model

2.2.1. Temporal Simulation of Rainfall

The intensity duration frequency (IDF) relationships was calculated based on the statistical analysis of point rainfall data from the meteorological stations collected over a long period of approximately several decades [27]. It varies in different cities. The statistical data can be used to calculate the relationships among the rainstorm return period, the rainfall intensity and the rainfall duration [28]. If there is a rainfall event that satisfies the characteristics of a specific rainstorm return period in the city, the formula can be used to approximate the average rainfall intensity at any time during the rainfall event. Then, the total rainfall over the entire rainfall area can be calculated by multiplying the average rainfall intensity by the rainfall duration.

For most cities in China, municipal models of IDF relationships characterizing local rainfall are frequently applied in engineering, particularly for municipal drainage design [29]. The precipitation, based on the contributing areas of depressions, can be calculated as:

$$P_w = A_w \times \int_0^t i dt \quad (2)$$

where P_w is the precipitation of the w catchment; A_w is the area of the w catchment; t is the rainfall duration time; and i is the local rainfall intensity.

2.2.2. Spatial Simulation of Rainfall

For large-area inundation simulation, the spatial variations of rainfall need to be considered, especially on the condition of lacking rainfall stations. Under the situation of the absence of urban rainfall station, the spatial distribution of rainfall needs to be simulated. Singh et al. [30] compared 13 different methods for estimating mean areal rainfall. There are three typical methods for simulating the spatial distribution of rainfall, including the isohyetal method, entropy, and a spatial interpolation method, such as kriging interpolation [31–33]. Distributed precipitation amounts between stations were interpolated for each time slice via ordinary kriging [34]. If the study area is small, spatial simulation is usually not used.

2.3. Surface Runoff Model

Due to the water balance law, the falling water will be drained in four ways, including infiltration, evaporation, surface runoff and sewer system runoff. Apirumanekul [35] proposed that evaporation per unit area makes up only 0.5% of the total rainfall volume from a three-day storm event in an urban environment. Therefore, the evaporation process is ignored in this study. Inundation in an urban area is entirely due to surface runoff.

2.3.1. Total Runoff Model

The Soil Conservation Service (SCS) model proposed by the United States Department of Agriculture (USDA) in 1954 has been used here to obtain the total runoff [36,37]. The formula is as follows:

$$Q = \begin{cases} \frac{(P-I_a)^2}{(P+S_m-I_a)} & P \geq I_a \\ 0 & P < I_a \end{cases} \quad (3)$$

$$S_m = \frac{25,400}{CN} - 254 \quad (4)$$

where Q is the total runoff; P is the amount of precipitation; I_a is the initial abstraction; and S_m is the maximum potential soil moisture retention. The relationship between I_a and S_m ($I_a = 0.2 S_m$) was developed by analyzing rainfall-runoff data from many small watersheds. The USDA uses the runoff curve number (CN) to determine the parameter S_m as in formula (4).

2.3.2. Sewer System Runoff

Sewer system runoff is another important part of the water balance law in urban areas. Underground drainage pipelines make up the most important drainage system of a city and the effect of sewer network influences inundation a lot in the urban area. Therefore, the sewer system plays an important role in SUSIM. For most cities in China, municipal models of IDF relationships characterizing local rainfall are frequently applied in engineering, particularly in municipal drainage design [38]. The municipal drainage design is used to estimate the average velocity of water drainage during the rainfall-runoff event. Then, the drainage water of one pipe can be estimated by its average velocity of water drainage multiplied by the storm duration.

All drainage pipes will be divided into different drainage regions according to the distribution of drainage pipes. The spatial drainage region division method groups all drainage pipes in one contributing area of depression into a single drainage region. Thus, the total displacement of each catchment can be calculated by the following equation:

$$Q_{pipe} = \sum_{i=1}^k q_i t \quad (k = 1, 2, 3 \dots k) \quad (5)$$

where Q_{pipe} is the total displacement of one catchment, q_i is the average velocity of water drainage of pipe i , t is the storm duration and k is the total number of pipes in this catchment.

2.4. Inundation Model

2.4.1. Urban Surface Runoff Calculation

In this study, the contributing areas of depressions are the smallest hydrologic units that do not exchange water with one another. The final surface runoff of one catchment is equal to the difference between the total runoff and the total displacement in it. Therefore, the surface runoff for a catchment can be calculated as follows:

$$S_w = \sum_{i=1}^m \sum_{j=1}^n (Q_w - Q_{pipe(w)}) \times A \times Z_{ij} \quad (i = 1, 2, \dots, m; j = 1, 2, \dots, n) \quad (6)$$

where S_w is the surface runoff of the w catchment, Q_w is the total runoff of the w catchment, $Q_{pipe(w)}$ is total displacement the w catchment, A is the area of grid cell and Z_{ij} is the weighted value (if Z_{ij} belongs to the w catchment, then $Z_{ij} = 1$; or $Z_{ij} = 0$).

2.4.2. Urban Inundation Distribution

To determine the distribution of the inundation, the direction of flow needs to be calculated first. The direction of flow is determined by the direction of the maximum drop from each unit. This is calculated by the following equation:

$$\text{Maximum drop} = \text{change in } z \text{ value} / \text{distance} \times 100 \quad (7)$$

The distance is calculated between cell centers. Therefore, if the cell size is 1, the distance between two orthogonal cells is 1 and the distance between two diagonal cells is 1.414 (the square root of 2). If the maximum descent between several cells is the same, the neighborhood is enlarged until the steepest descent is found. When a direction of steepest descent is found, the output cell is coded with the value representing that direction. The flow direction raster will show values of 1, 2, 4, 8, 16, 32, 64, or 128 in its eight directions. The process to determine the direction of flow is shown in Figure 2.

Then, the flow direction raster can be used to calculate the real state of inundation. The flow direction will assign the excess water from high elevation cell to a lower elevation with its adjacent grid cell. The cells in which flooding depth exceeds 0.001 m are defined as source cells (we assume that if two grids have a flooding depth under 0.001 m, they will not change water with each other). As Figure 3 shows, all the grids need to go round and be judged. The excess water will accumulate in the downstream catchments and the inundation distribution can be determined.

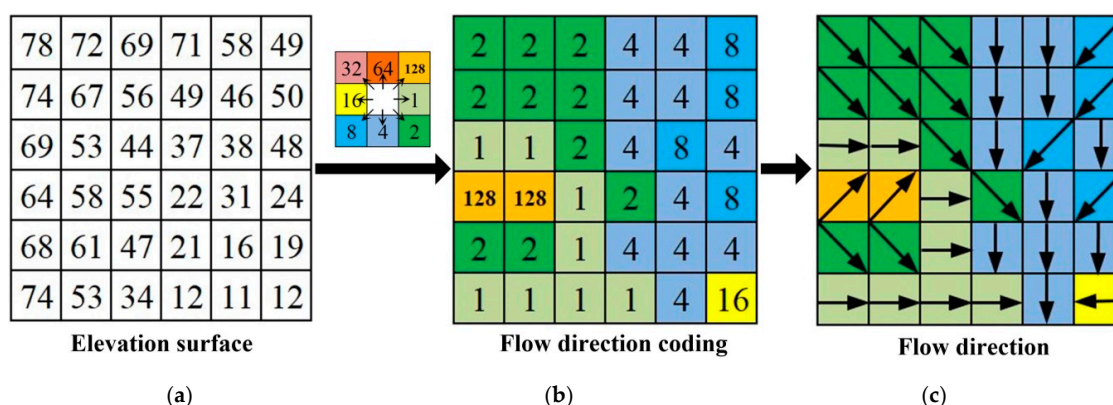


Figure 2. The process of obtaining flow direction. (a) elevation surface; (b) flow direction coding; (c) flow direction.

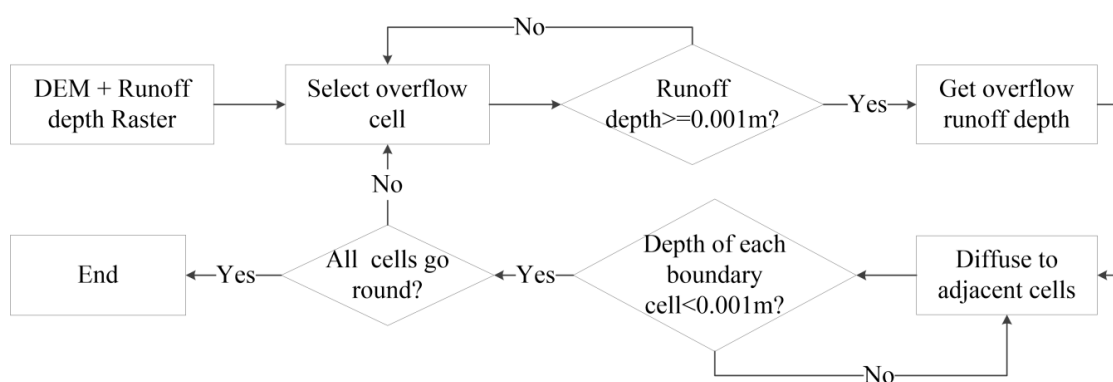


Figure 3. The process of inundation diffusion.

3. Case Study

3.1. Study Area

Haining City is located in Zhejiang province, southeast China from 30°15′–30°35′ N and 120°18′–120°52′ E. The city experiences a subtropical monsoon climate in which increased precipitation and high temperatures during the same period. There are two periods of concentrated rainfall each year in Haining, namely, the plum rain season in June–July and the typhoon season in July–September, which combine to account for an annual average precipitation of 1187 mm. The excessive concentration of rain during the flood season has led to the aggravation of urban storm water flooding. In addition, the rapid urbanization, the reduction in urban green spaces, the increase in the impervious surface area and the inadequate infrastructure all contribute to the waterlogging that occurs frequently during the rainy seasons.

The central urban area of Haining (Figure 4) includes the Haining First High School, the China Leather Mall, the West Mountain Park and other residential districts, with the total area of 5.9 km². It is the political, economic and cultural center of Haining. In addition, this area is one of the regions in Haining that is most often damaged by urban inundation. Some locations such as Wenyuan and Haining Avenue frequently have extensive areas of inundation. This area is surrounded by a network of rivers and roads, making it difficult for outside water to flow in and to exchange with the internal water. Therefore, it is selected as the study area in which to simulate storm inundation.

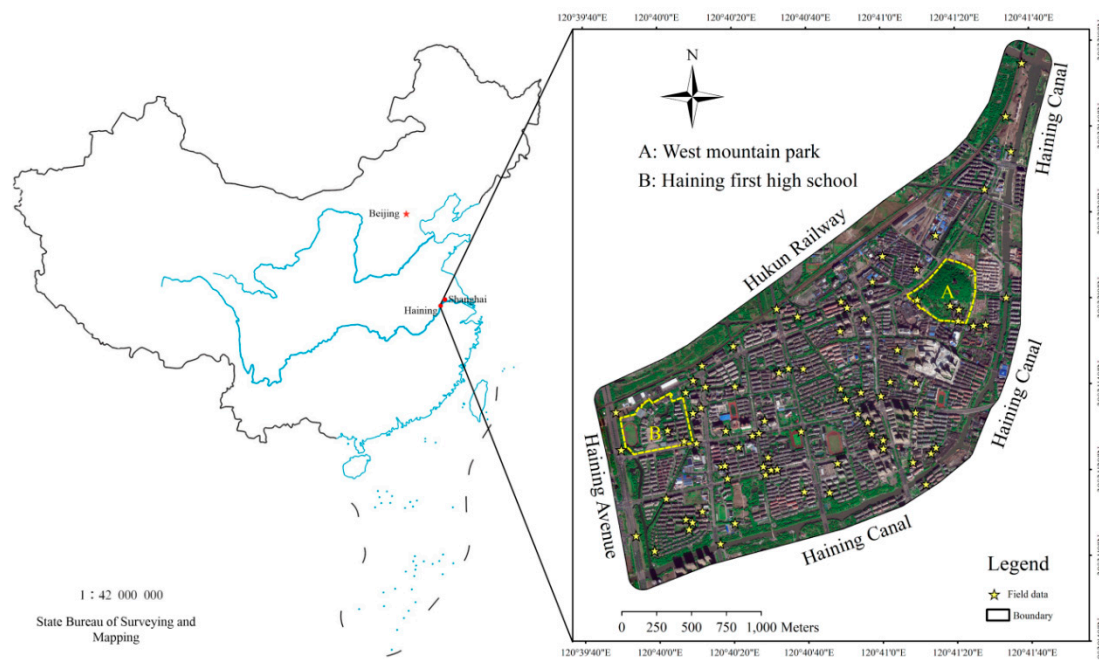


Figure 4. Study area.

3.2. Data Descriptions

3.2.1. Digital Elevation Model (DEM) Acquisition

The DEM data provided by the Zhejiang Administration of Surveying Mapping and Geoinformation (ZASMG) is used in this study case with a 2 m resolution. It is processed and quality controlled by ZASMG by using digital surface model (DSM). The DSM was created from light laser detection and ranging (LiDAR) point data with a point density of 0.2 m. After noise removal, system error correction, surface laser spot classification, smoothing and resample, the DEM of 2 m grid can be obtained. As shown in Figure 5a, the highest point in study area is in the West Mountain Park.

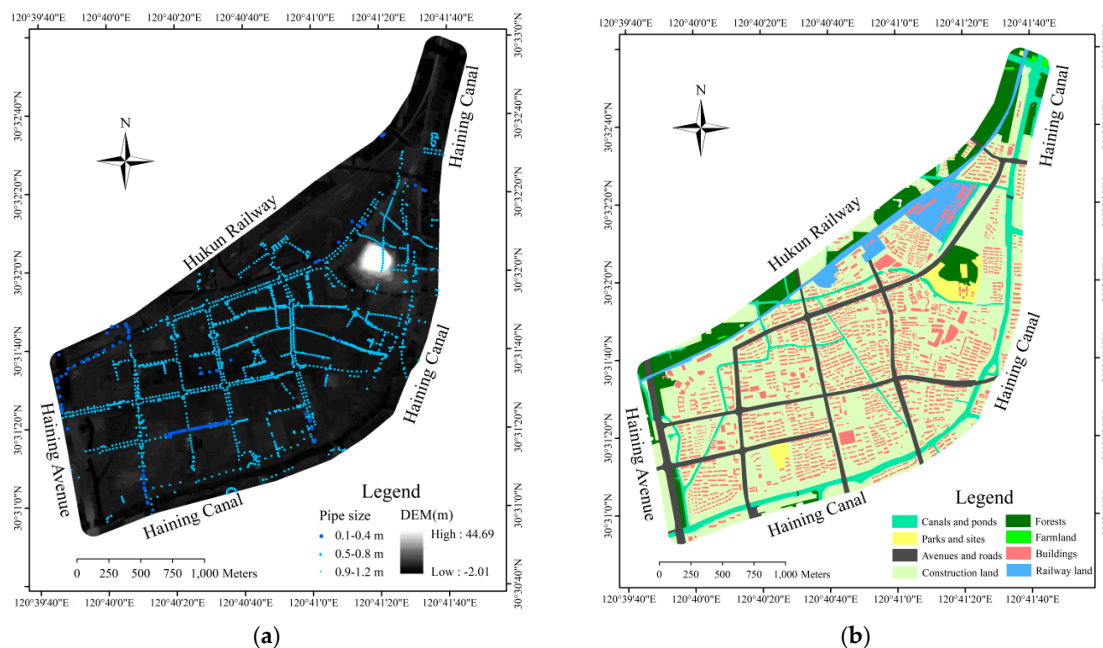


Figure 5. Data description. (a) digital elevation model (DEM) and sewer network data; (b) land-use map.

3.2.2. High-Resolution Image and Land-Use Map

The high-resolution image is an unmanned aerial vehicle (UAV) image with a 0.5 m spatial resolution. The image was acquired on 26 October 2016. There are three main steps to preprocess a UAV image. First, the image is defined with the Universal Transvers Mercator projection (UTM Zone 50N) and the WGS84 datum. Second, it is carefully georeferenced using a 1st-order polynomial transformation method so that its root mean squared error is under 2 pixels. Third, it is clipped to the same extent as the DEM. The image is shown in Figure 4.

In general, different types of land use have different CN values, and therefore the land-use map is necessary for estimating the CN value. The basic land-use data were from ZASMG and were rectified again by the UAV image and a field survey. In this study, land use types are divided into 8 types of secondary classifications (canals and ponds, parks and sites, construction land, avenue and road, railway land, forests, farmland, buildings). Using a combination of computer automatic classification and human-computer interaction for land-use extraction, we interpreted and mapped the study area for the year 2016. The land-use map is shown in Figure 5b.

3.2.3. Precipitation Data

Three well documented rainstorms which were the most intense storm events during the year 2017 (25 June 2017; 26 August 2017 and 20 September 2017) were selected for model simulation and validation. All data are from the nearest Bianshi Precipitation Station (approximately 2 km away from the center of the study area). On 25 June, rainfall was heavy from 9:00 to 11:00. The storm was highly concentrated and intense, the rainfall amount in the first hour accounted for over 80% of the total for that day. Thus, the first hour of this storm event (9:00 to 10:00), approximately 52 mm/h, was used as the input rainfall data. On 26 August, it has the highest intense rain of this month from 12:00 to 13:00 for about 47 mm/h. On 20 September, the storm event from 18:00 to 19:00 was forecasted as the heaviest rainfall of this month. Therefore, the precipitation data (55 mm/h) and the field sampling data were collected and documented to verify SUSIM. The spatial rainfall simulation will not be considered in this study case due to the small extent.

The IDF formula for the Haining rainstorm was developed by the Meteorological Bureau of Zhejiang Province using forty-three years of rainfall records from 1963 to 2006. It can be represented by the following equation:

$$i = \frac{10.101 + 10.675 \log P}{(t + 11.30)^{0.682}} \quad (8)$$

where i is the rainfall intensity of Haining, P is the return period and t is the duration of rainfall. According to the IDF formula of Haining, the rainfall intensities with the duration of one hour and the 5-, 10-, 20- and 50-year return periods were formulated for the inundation projection after model validation.

3.2.4. Sewer Network Data

The sewer network data for Haining city were obtained from ZASMG and are shown in a geographic information system (GIS)-based dataset. The dataset contains approximately 4133 flood pipes, 8731 waste water pipes and 30,767 rainfall pipes. Each record in the GIS attribute table is associated with one drainage pipe in the city and characteristic information is recorded, such as detailed geographic and geometric information, the cross-sectional area of the pipe and average velocity of water drainage. All the sewer data have been further calibrated to match the DEM and the high-resolution image by a georeferencing tool based on ArcGIS. All these pipes and manholes can be used to drain water. Most of the pipes are circular, with diameters ranging from 0.1 to 4 m, while some pipes are rectangular with widths and heights varying from 0.4 to 3 m and from 0.6 to 4 m, respectively. A total of 8953 pipes and manholes were extracted for the simulation of the study area. The sewer pipes are shown in Figure 5a.

3.2.5. Field Data Collection

Field surveys were conducted on those three different rainy days in 2017 (25 June, 26 August and 20 September). A total of 80 ground samples (Figure 4) were randomly set in the study area. A portable global positioning system (GPS) was used to record coordinates of the plot center of the sample location. At each sampling plot, the depths of inundation were measured manually. The measured depth is the average inundation depth on each survey point.

3.3. Method

The study followed the following steps: (1) model running; (2) model validation and (3) inundation projection. The flowchart is shown in Figure 6.

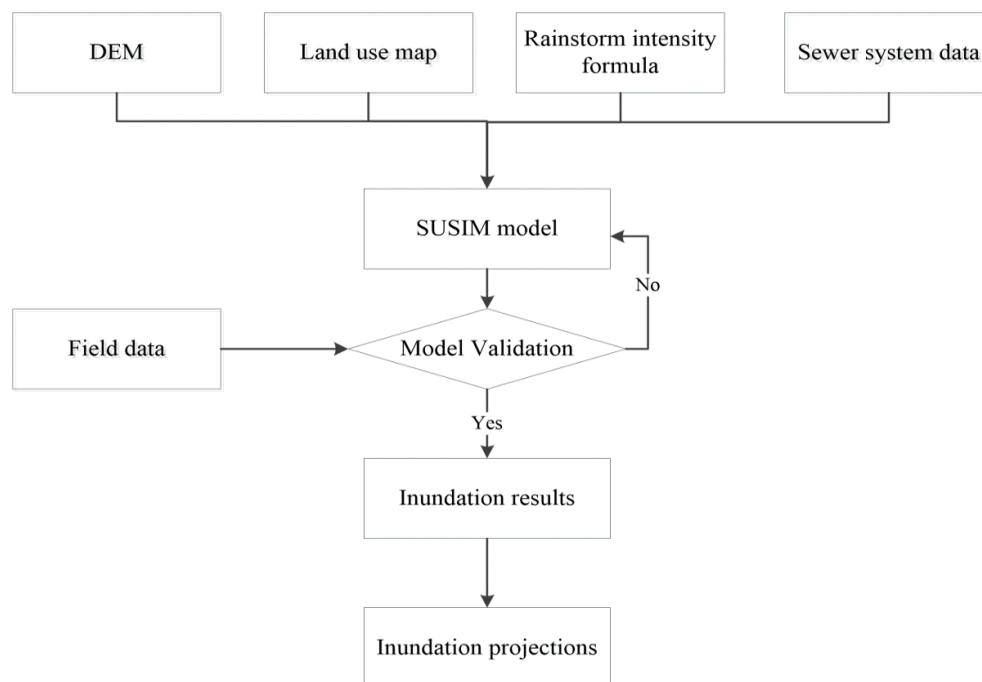


Figure 6. Flowchart of the simplified urban storm inundation model (SUSIM) model.

3.3.1. Model Running

The SUSIM model runs according to the following steps:

- First, for the urban terrain model, the parameter A in formula (1) can be set as a fixed value of 10 according to the mean height of the buildings in study area which is approximately 10 m. Then, the contributing areas of depressions can be acquired from the modified urban terrain.
- Second, for the total runoff model, construction land, avenue and road, railway land, buildings are the impermeable land area. Their area is approximately 4.13 km² and the CN of them is set as 90.8. CN of canals and ponds (water body) is set as 98. CN of parks and sites (low-density urban area) is set as 74. CN of farmland and forests are 78 and 55 separately. A CN raster map of the study area can be calculated from the land-use map (Figure 5b) based on GIS analysis. The potential maximum soil moisture retention S_m can be calculated by Equation (4) based on CN values. Thus, the total runoff is calculated by combining the precipitation data and the SCS model.
- Third, the drainage model is built based on the sewer system data according to the Equation (5). The surface runoff can be calculated by the total runoff and drainage model.
- Finally, the surface runoff is combined with the inundation diffusion process to obtain the final inundation results.

3.3.2. Model Validation

The accuracy of the SUSIM model was validated against those three actual inundation events (25 June 2017, 26 August 2017 and 20 September 2017). The coefficient of correlation is used here as a statistical indicator of the relationship between variables. There are total 80 field survey points with the simulated inundation depth and the measured inundation depth for the validation of each storm event.

3.3.3. Inundation Projections

After validation, if the accuracy is satisfactory, different rainstorm return period scenarios are simulated. The purpose of testing different scenarios is to predict the inundation depth and spatial distribution of flooding in Haining from different storms; therefore, such predictions can provide suggestions for inundation monitoring and management. The rainfall intensities for one hour and the 5-, 10-, 20- and 50-year return periods can be calculated for the subsequent scenario analyses. The four steps to finish the inundation projections under different scenarios are described below.

First, the rainfall intensity under different scenarios is calculated by Equation (8). Second, the total runoff under different scenarios is calculated based on the SCS model and the total displacement of each catchment can be calculated by Equation (4). Third, the surface runoff of different rainfall intensity is calculated according to Equation (6). Finally, the inundation depth is simulated by SUSIM.

3.4. Results

3.4.1. Urban Terrain and Catchment Modification Results

Using Equation (8), the building profiles were distinguished from the original DEM. The modified DEM layer is shown in Figure 7a. Then, the catchments were acquired using the modified DEM, based on the hydrology tools in ArcGIS. The contributing area of depressions and the drainage capacity of each catchment are shown in Figure 7b.

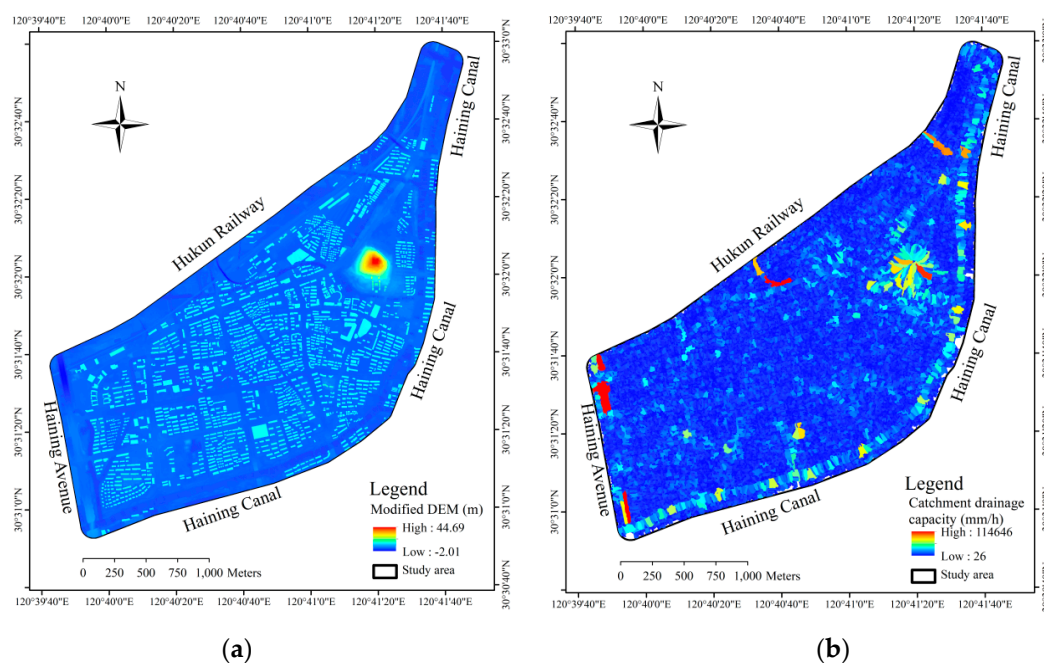


Figure 7. Urban terrain and catchment modification results. (a) urban terrain modification results; (b) catchments and their drainage capacities.

The accuracy of the DEM was greatly improved by considering the block effects of the buildings. As shown in Figure 7b, there are totally 25,863 catchments in the study region. The drainage capacity of each catchment can be calculated by Equation (5). The red to blue colors show the drainage capacity.

3.4.2. Inundation Results

The inundation results for 25 June 2017, 26 August 2017 and 20 September 2017 have been simulated based on the SUSIM model. The surface runoff of each catchment was calculated by Equations (3)–(6) using the input rainfall data (52 mm/h, 47 mm/h, 55 mm/h) based on GIS analysis. Then, the amount of excess water in each catchment was redistributed according to the inundation model. The inundation results are presented in Figure 8.

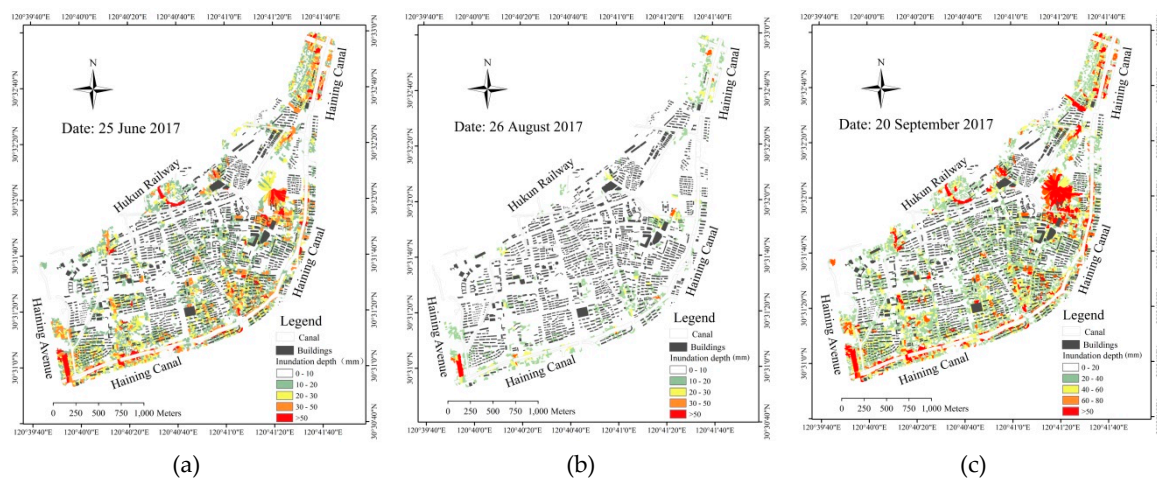


Figure 8. Simulated inundation results. (a) 25 June 2017; (b) 26 August 2017; (c) 20 September 2017.

Haining Avenue, West Mountain Park and the old urban area in the northeast part of the city would encounter the most extensive and severe inundation, according to the simulation results. The survey point with the most severe inundation, almost 160 mm, is on Haining Avenue.

3.4.3. Validation Results

These three simulation results were compared to the field survey data and plotted in Figure 9. Each correlation coefficient is higher or equal to 0.75. The precision is high and the simulation results are credible. The comparison results were consistent, which indicates that the model can be used to simulate different scenarios for Haining.

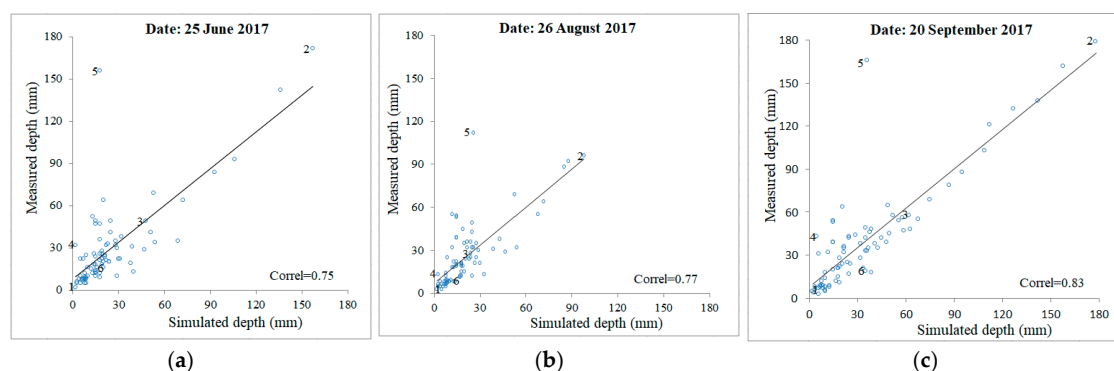


Figure 9. Plots of validation points. (a) 25 June 2017; (b) 26 August 2017; (c) 20 September 2017.

Six typical sample data groups were selected and are shown in Table 1. From point.1 to point.6, these sample points are the railway station, Haining Avenue, West Mountain Park, Haining First High School, the underground garage and the police station, respectively. Detailed information, including the location (longitude and latitude) and the simulated and measured results are shown in Table 1.

Table 1. Comparison of the simulated and measured inundation results of six sample data (Depth unit: mm).

No.	Survey Points	25 June		26 August		20 September		Longitude/E	Latitude/N
		M	S	M	S	M	S		
1	Railway station	4	5.6	3	2.8	7	6	120°39'11"	30°31'11"
2	Haining Avenue	178	160	96	98	178	179.5	120°40'05"	30°31'13"
3	West Mountain Park	44	47	26	29	62	58	120°40'19"	30°31'11"
4	Haining first high school	2	32	3	13	5	43	120°41'33"	30°31'08"
5	Underground garage	162	18	116	26.9	167	36	120°40'31"	30°31'24"
6	Police station	20	16	13	8	21	34	120°40'35"	30°31'44"

M represents measured inundation results and *S* represents simulated inundation results. Year: 2017.

The maximum offsets of the three validation data are found on Point.4 and Point.5, as shown in Figure 9 and Table 1. For Point.4, the measured results are much lower than the simulated depths. The main reason is the limitation of the DEM spatial resolution. This filed point is near a small depression of 1 m². The DEM of two meters' resolution cannot show the accurate terrain change inside one cell. The terrain accuracy can affect the result a lot. For Point.5, the simulated results are much lower than the measured depths. The main reason for these discrepancies is that garages in study area are mainly built on the underground floor of buildings. Therefore, it is difficult to correct for these features during the terrain modification process. In order to get accurate results, the location and depth of the underground garages should be documented in the field survey plan. Their real depths need to be removed from the DEM.

3.4.4. Inundation Projections under Different Storm Scenarios

The predicted spatial and statistical results of the maximum inundations (extent and depth) in the simulations for different storm return periods are shown in Figure 10. The key parameters of the inundation results for the storms of 5-, 10-, 20- and 50-year return periods are shown in Table 2.

Table 2. Runoff and inundation data under different storm scenarios.

Return Period (Year)	5	10	20	50
Rainfall intensity (mm/h)	58	67	77	91
Maximum inundation depth(mm)	403	812	1233	1522
Maximum inundation area (m ²)	2904	4675	5051	7330

As the storm return period increases from 5-year to 50-year, the maximum inundation depths are significantly increased from 403 mm to 1522 mm and the maximum inundation area increased from 2904 m² to 7330 m². Among these different storm scenarios, Haining Avenue experienced the first and most severe inundation for 1 h duration storm. The results of the complex inundation states that occur under different storm return periods are shown in Figure 10.

In the 5-year return period scenario (Figure 10a), the most severe inundation occurs on Haining Avenue, especially on the southern part of the avenue. The lack of drainage pipes and the low terrain are probably the main reasons for the inundation severity.

In the 10-year return period scenario (Figure 10b), severe inundation occurs in West Mountain Park. The depths of inundation in the sub catchments of the park are mainly from 0.3 m to 0.5 m. This is possibly due to the park's dense vegetation which can hold water and somewhat hinder the normal dissipation of accumulated rainfall. The complex terrain of the park also restricts the rainfall from

draining outside of the park. Additionally, most of the drainage networks of the West Mountain Park are outside the park and it lacks drainage points inside the park, which also restricts its drainage ability.

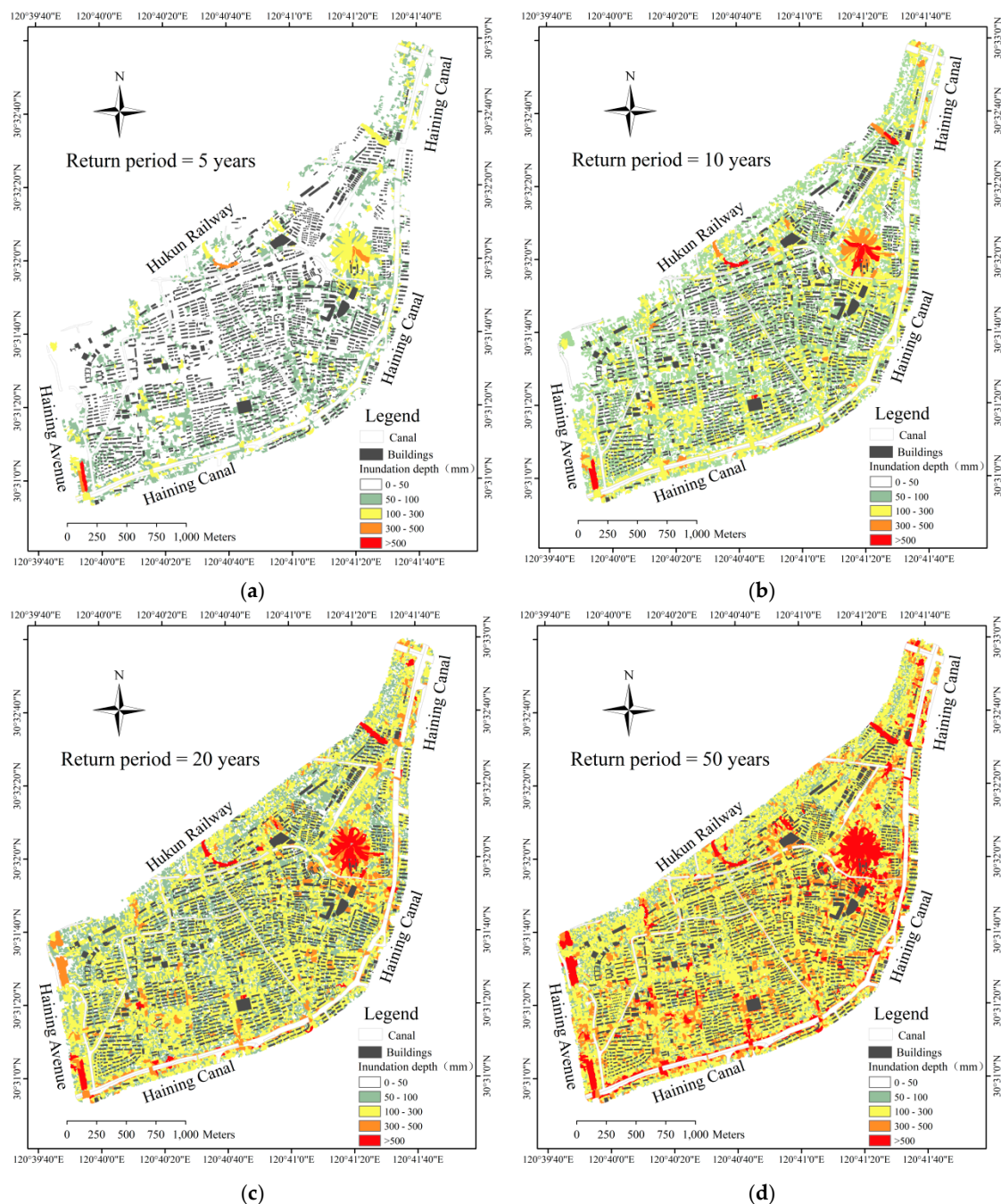


Figure 10. Projected inundation depths under four storm scenarios. (a) return period = 5 years; (b) return period = 10 years; (c) return period = 20 years; (d) return period = 50 years.

In the 20-year return period scenario (Figure 10c), the depths of inundation are greater than 0.5 m in the northeast corner of the study area. These areas are the old residential parts of the old urban area and were constructed approximately 60 years ago. The inundation mainly results from unreasonable planning and old drainage facilities. The drainage pipes in the areas that experienced the worst inundation are smaller than those in other places such as the new construction areas in the middle part of the study area. Therefore, it is suggested that the drainage facilities in old city are reconstructed.

In the 50-year return period scenario (Figure 10d), the study area is almost entirely flooded. The floodwater gradually spreads to the lower catchments. The most severe inundations are along the roads, pathways, and in some lowlands, especially in underground garages in the residential areas.

4. Discussion

4.1. Advancement and Sensitivity of the Simplified Urban Storm Inundation Model (SUSIM)

A simple and effective model called SUSIM has been proposed in this paper. It has a simple model structure and considers the complicated urban terrain. The distribution of urban inundation can be simulated easily and accurately based on the proposed model. A modified DEM was used as the model input and the contributing area of depressions were used as the basic study units of SUSIM; these units can accurately reflect the real urban terrain and hydrological environment. The total runoff of each catchment can be calculated easily based on SUSIM by using Equation (3). Setting the drainage capacity by generalizing the sewer network by using Equation (5) makes the simulation process simpler. The correlation coefficients are higher or equal to 75% of 3 historical rainstorm validation cases, indicating that the model performs well in all these actual events and can help to deal with location-specific flooding problems.

The precision of the DEM and accurate inundation model are the key factors of SUSIM. The modified DEM layer fully considered the impact of the detailed urban terrain on storm runoff and flooding processes. This paper only approximates the constructed parts of the city; however, the real urban terrain is very complicated. Many factors need to be considered, such as roads, river networks, underground spaces, urban landscapes and so on. To improve the authenticity and reliability of scenario simulations, future research will focus on modifying the urban terrain by considering more complex surface information like underground garages.

4.2. Limitations of the SUSIM

SUSIM also has several limitations. First, the parameters of SUSIM are not universal and need to be adjusted according to the specific study area. All parameters need to be set separately according to the actual conditions of the study area. In addition, the process of determining parameters is complicated and the data are difficult to acquire. For example, the parameters of the SCS model, such as the CN, are affected by complicated factors and every factor can greatly affect the accuracy; for example, the drainage capacity parameters are affected by sewer network designs in different cities. However, the sewer data are difficult to collect. Second, the lack of verification in large areas is another limitation. In the case study, the study area is small and the rainfall model of SUSIM is further simplified. Therefore, more data need to be collected and the study area needs to be expanded appropriately in the future. The parameters of SUSIM will be calibrated and corrected again to further improve the accuracy of the model. Third, like many other simplified inundation models such as GIS-based urban flood inundation model (GUFIM), urban storm-inundation simulation method (USISM), RFSM and so on, SUSIM is only a flat water model and is not a physically based dynamic model; therefore, it can only calculate the final inundation state of a storm and cannot show the inundation process itself.

5. Conclusions

This paper has presented a simplified urban storm inundation model, SUSIM, which simulates urban inundation. The case study presented uses the central urban area of Haining, China, as the study area in which to simulate the conditions of storm inundation. The simulation results are tested and validated by the field survey data. The validation results show that the model accuracy is satisfactory. Finally, four levels of rainfall intensity (with 5-, 10-, 20- and 50-year return periods, respectively) are considered and simulated. Although we selected Haining City as a case study to verify the SUSIM, the model may also be transferable to other regions. This transferability is due to the method's

simplified distributed hydrologic model, which is based on improved DEM and catchments and, therefore, is more suitable for urban areas.

The main conclusions are summarized as follows:

1. DEM, as the basic model input, needs to accurately reflect the real urban terrain. A modified DEM is derived from the original DEM by considering the impact of buildings blocking the flow of water. In addition, canals and streets are considered in the modification. In addition, the contributing areas of depressions are the basic study units of SUSIM and are generated from the modified DEM and can accurately reflect the urban terrain.
2. The SUSIM model has fast simulations and its results are acceptable, as indicated by the high coefficient of correlation ($\geq 75\%$) of three historical storm validations. The validations showed that this study will be beneficial for urban planning and emergency preparation.
3. Scenario analysis demonstrates a high degree of consistency in the inundation patterns among the 5-, 10-, 20- and 50-year storms. Haining Avenue, West Mountain Park, and the old residential part of the city experience the most severe inundations under these scenarios. Haining Avenue has high inundation risk for its low elevation (the lowest part of Haining Avenue is just -1.82 m). The reasons for inundation in the old residential area are its low elevation with an elevation of -0.88 m in the lowest part and old drainage facilities that constructed about 40 years ago. These low-elevation places are suggested to be rebuilt. For the places like West Mountain Park that lack drainage facilities, it is suggested that the drainage network is redesigned and extended.
4. Due to hydrological variability, which is driven by complicated factors, urban inundation is becoming less predictable and more complicated with enlarging uncertainties.

Author Contributions: Y.L. performed the experiments and wrote the paper; and T.H. designed the research and revised the paper. G.Z. provided data and substantial comments; L.S. and J.F. undertook the field survey and wrote the validation part; D.Z. extensively edited the paper. All authors commented on and approved the final manuscript.

Funding: This research was funded by the National Natural Science Foundation of China (Grant No. 41676167); the Zhejiang Provincial Natural Science Foundation of China (Grant No. LY19D010004) and the Science and Technology Program of Hangzhou (Grant No. 20191203B19).

Conflicts of Interest: The authors declare no conflict of interest.

References

1. Zhang, S.; Pan, B. An urban storm-inundation simulation method based on GIS. *J. Hydrol.* **2014**, *517*, 260–268. [[CrossRef](#)]
2. Miller, J.D.; Hess, T. Urbanisation impacts on storm runoff along a rural-urban gradient. *J. Hydrol.* **2017**, *552*, 474–489. [[CrossRef](#)]
3. Huang, Q.; Wang, J.; Li, M.; Fei, M.; Dong, J. Modeling the influence of urbanization on urban pluvial flooding: A scenario-based case study in Shanghai, China. *Nat. Hazards* **2017**, *87*, 1035–1055. [[CrossRef](#)]
4. Wu, X.; Wang, Z.; Guo, S.; Liao, W.; Zeng, Z.; Chen, X. Scenario-based projections of future urban inundation within a coupled hydrodynamic model framework: A case study in Dongguan City, China. *J. Hydrol.* **2017**, *547*, 428–442. [[CrossRef](#)]
5. Jiang, X.; Yuan, H.; Xue, M.; Chen, X.; Tan, X. Analysis of a heavy rainfall event over Beijing during 21–22 July 2012 based on high resolution model analyses and forecasts. *J. Meteorol. Res.* **2014**, *28*, 199–212. [[CrossRef](#)]
6. Liu, C.; Li, Y. GIS-based dynamic modelling and analysis of flash floods considering land-use planning. *Int. J. Geogr. Inf. Sci.* **2016**, *31*, 481–498. [[CrossRef](#)]
7. Zhu, Z.; Chen, Z.; Chen, X.; He, P. Approach for evaluating inundation risks in urban drainage systems. *Sci. Total Environ.* **2016**, *553*, 1–12. [[CrossRef](#)]
8. Teng, J.; Jakeman, A.J.; Vaze, J.; Croke, B.F.W.; Dutta, D.; Kim, S. Flood inundation modelling: A review of methods, recent advances and uncertainty analysis. *Environ. Model. Softw.* **2017**, *90*, 201–216. [[CrossRef](#)]

9. Amaguchi, H.; Kawamura, A.; Olsson, J.; Takasaki, T. Development and testing of a distributed urban storm runoff event model with a vector-based catchment delineation. *J. Hydrol.* **2012**, *420–421*, 205–215. [[CrossRef](#)]
10. Rogers, C.C.M.; Beven, K.J.; Morris, E.M.; Anderson, M.G. Sensitivity analysis, calibration and predictive uncertainty of the institute of hydrology distributed model. *J. Hydrol.* **1985**, *81*, 179–191. [[CrossRef](#)]
11. Rossman, L.A. *Storm Water Management Model User's Manual Version 5.1*; USEPA: Washington, DC, USA, 2014.
12. Bai, Y.; Zhao, N.; Zhang, R.; Zeng, X. Storm water management of low impact development in urban areas based on SWMM. *Water*. **2018**, *11*, 33. [[CrossRef](#)]
13. Gassman, P.W.; Sadeghi, A.M.; Srinivasan, R. Applications of the SWAT model special section: Overview and insights. *J. Environ. Qual.* **2014**, *43*, 1–8. [[CrossRef](#)] [[PubMed](#)]
14. Abbaspour, K.C.; Rouholahnejad, E.; Vaghefi, S.; Srinivasan, R.; Yang, H.; Klöve, B. A continental-scale hydrology and water quality model for Europe: Calibration and uncertainty of a high-resolution large-scale SWAT model. *J. Hydrol.* **2015**, *524*, 733–752. [[CrossRef](#)]
15. Bruwier, M.; Archambeau, P.; Erpicum, S.; Piroton, M.; Dewals, B. Shallow-water models with anisotropic porosity and merging for flood modelling on Cartesian grids. *J. Hydrol.* **2017**, *554*, 693–709. [[CrossRef](#)]
16. Guinot, V.; Sanders, B.F.; Schubert, J.E. Dual integral porosity shallow water model for urban flood modelling. *Adv. Water Resour.* **2017**, *103*, 16–31. [[CrossRef](#)]
17. Jang, S.; Cho, M.; Yoon, J.; Yoon, Y.; Kim, S.; Kim, G.; Kim, L.; Aksoy, H. Using SWMM as a tool for hydrologic impact assessment. *Desalination* **2007**, *212*, 344–356. [[CrossRef](#)]
18. Hsu, M.H.; Chen, S.H.; Chang, T.J. Inundation simulation for urban drainage basin with storm sewer system. *J. Hydrol.* **2000**, *234*, 21–37. [[CrossRef](#)]
19. Li, Y.; Hu, T.; Pan, X.; Lei, X. Research progress on disaster simulation and risk assessment for urban waterlogging. *Geo.World* **2017**, *2*, 42–49. (In Chinese)
20. Krupka, M.; Wallis, S.; Pender, S.; Neélz, S. Some practical aspects of flood inundation modelling. Transport phenomena in hydraulics, publications of the institute of geophysics. *Pol. Acad. Sci.* **2007**, *7*, 129–135.
21. Leandro, J.; Schumann, A.; Pfister, A. A step towards considering the spatial heterogeneity of urban key features in urban hydrology flood modelling. *J. Hydrol.* **2016**, *535*, 356–365. [[CrossRef](#)]
22. Chen, J.; Hill, A.A.; Urbano, L.D. A GIS-based model for urban flood inundation. *J. Hydrol.* **2009**, *373*, 184–192. [[CrossRef](#)]
23. Zhang, S.; Wang, T.; Zhao, B. Calculation and visualization of flood inundation based on a topographic triangle network. *J. Hydrol.* **2014**, *509*, 406–415. [[CrossRef](#)]
24. Coveney, S.; Fotheringham, A.S. The impact of DEM data source on prediction of flooding and erosion risk due to sea-level rise. *Int. J. Geogr. Inf. Sci.* **2011**, *25*, 1191–1211. [[CrossRef](#)]
25. Saksena, S.; Merwade, V. Incorporating the effect of DEM resolution and accuracy for improved flood inundation mapping. *J. Hydrol.* **2015**, *530*, 180–194. [[CrossRef](#)]
26. Rieger, W. A phenomenon-based approach to upslope contributing area and depressions in DEMs. *Hydrol. Process.* **1998**, *12*, 857–872. [[CrossRef](#)]
27. Soltani, S.; Helfi, R.; Almasi, P.; Modarres, R. Regionalization of rainfall intensity-duration-frequency using a simple scaling model. *Water Resour. Manag.* **2017**, *31*, 4253–4273. [[CrossRef](#)]
28. Zhao, S.; Chen, Z.; Xiong, L. Establishment of simplified urban waterlogging model using spatial analysis. *J. Nat. Disasters* **2004**, *13*, 8–14. (In Chinese)
29. Yin, Z.; Yin, J.; Xu, S.; Wen, J. Community-based scenario modelling and disaster risk assessment of urban rainstorm waterlogging. *J. Geogr. Sci.* **2011**, *21*, 274–284. [[CrossRef](#)]
30. Singh, V.P.; Chowdhury, P.K. Comparing some methods of estimating mean areal rainfall. *J. Am. Water Resour. Assoc.* **1986**, *22*, 275–282. [[CrossRef](#)]
31. Chen, Y.; Wei, C.; Yeh, H. Rainfall network design using kriging and entropy. *Hydrol. Process.* **2008**, *22*, 340–346. [[CrossRef](#)]
32. Xu, P.; Wang, D.; Singh, V.; Wang, Y.; Wu, J.; Wang, L.; Zou, X.; Liu, J.; Zou, Y.; He, R. A kriging and entropy-based approach to raingauge network design. *Environ. Res.* **2018**, *161*, 61–75. [[CrossRef](#)] [[PubMed](#)]
33. Kebaili Bargaoui, Z.; Chebbi, A. Comparison of two kriging interpolation methods applied to spatiotemporal rainfall. *J. Hydrol.* **2009**, *365*, 56–73. [[CrossRef](#)]
34. Yin, J.; Yu, D.; Wilby, R. Modelling the impact of land subsidence on urban pluvial flooding: A case study of downtown Shanghai, China. *Sci. Total Environ.* **2016**, *544*, 744–753. [[CrossRef](#)] [[PubMed](#)]

35. Apirumanekul, C. Modelling of Urban. Flooding in Dhaka City. Master's Thesis, Asian Institute of Technology, Bangkok, Thailand, 2001.
36. Boughton, W.C. A review of the USDA SCS curve number method. *Soil Res.* **1989**, *27*, 511–523. [[CrossRef](#)]
37. Mishra, S.K.; Singh, V.P. Soil Conservation Service Curve Number (SCS-CN) Methodology. *Water Sci. Technol. Libr.* **2003**, *22*, 355–362.
38. Yin, J.; Yu, D.; Yin, Z.; Liu, M.; He, Q. Evaluating the impact and risk of pluvial flash flood on intra-urban road network: A case study in the city center of Shanghai, China. *J. Hydrol.* **2016**, *537*, 138–145. [[CrossRef](#)]



© 2019 by the authors. Licensee MDPI, Basel, Switzerland. This article is an open access article distributed under the terms and conditions of the Creative Commons Attribution (CC BY) license (<http://creativecommons.org/licenses/by/4.0/>).